

We are grateful to you for the time you invested in providing detailed and helpful feedback. Your comments have been invaluable in refining and strengthening our manuscript.

As a general clarification, we updated the station names for Nuup Kangerlua from GF6, GF7, etc., which referenced the Danish name Godthåbsfjord, to NK6, NK7, etc., to more clearly reflect their association with Nuup Kangerlua and enhance consistency throughout the manuscript.

We therefore added:

Line 137: It is important to note that earlier studies (e.g., Mortensen et al., 2011, 2014, 2018; Meire et al., 2015, 2017; Stuart-Lee et al., 2021, 2023) referred to the same stations in Nuup Kangerlua using the prefix “GF”, derived from the Danish name “Godthåbsfjord”. In this study, we use the prefix “NK” instead, to reflect the Greenlandic name “Nuup Kangerlua”.

To avoid confusion, we updated this naming (NK) in your comments as well. We also numbered your questions to structure our answers.

(1) In Fig. A1, it looks as if 210PB_xs was very low (and almost constant) for e.g. NK13 and NK6, how were sedimentation rates derived there?

Following your comment, we chose to omit the sedimentation rate estimate of NK6, because (1) it is not a deep profile; only 10 cm deep and (2) $^{210}\text{Pb}_{\text{xs}}$ activity is indeed very low. This may be due to erosion conditions at the sill slope where older sediment material (characterized by low $^{210}\text{Pb}_{\text{ex}}$ activity) surfaces due to removal of younger sediment or older sediment has been transported to this location, which is also visible in NK7 and 9 profiles. The omission of the low MAR estimate at station NK6 resulted in a slightly higher average organic carbon burial rate for Nuup Kangerlua: $18.0 \pm 1.6 \text{ g m}^{-2} \text{ yr}^{-1}$ versus the previously calculated $14.1 \pm 1.6 \text{ g m}^{-2} \text{ yr}^{-1}$.

For station NK13 on the other hand, we opt to keep our estimate. MAR and SAR have been calculated the same way as for cores of stations AM10, NK12 and NK12 (see reply to question (3)). It is relatively close to the estimate of Pelikan et al. (2019) who sampled a sediment core at a distance of about 2.5 km west from our location, NK13. They estimated an age of ~200 years at the bottom of a 569 cm long sediment core, which comes down to an average sedimentation rate of ~2.85 cm yr⁻¹. Therefore, taking the lower SAR of 1.50 cm yr⁻¹ that we calculated would be more conservative. However, it should indeed be stressed in the manuscript that the MARs for stations NK13, NK12, NK10, AM10, which were obtained using the CF:CS calculation method, are less robust than the stations where the CSR method could be applied (as addressed in more depth in one of the answers below). Therefore we added: **Line 366:** “Note that the accumulation rates at stations NK10, NK12, NK13, and AM10 are estimates based on the CF:CS model and were not validated with independent time markers (Smith 2001; Barsanti 2020). Therefore, these estimates should be confirmed in future studies.”

Moreover, we recalculated the MARs obtained by CRS dating as we first took the arithmetical average of the MARs. However, this approach did not account for the fact that, because MARs were not constant, each sediment layer corresponds to a different time span and should therefore be assigned a different statistical weight. The simplest way to give an average MAR (or SAR) in CRS dating, is to calculate the ratio depth/age in a deep layer. Therefore, we chose layers where the ages calculated using $^{210}\text{Pb}_{\text{ex}}$ method were confirmed by the ^{137}Cs profiles, hence the average value during approximately the last 60 years:

AM5: A depth of $19 \pm 1 \text{ cm}$ or $5.45 \pm 0.25 \text{ g cm}^{-1}$ (2021-1966) corresponds to $55 \pm 2 \text{ years}$.

$$\text{MAR} = 1.0 \pm 0.1 \text{ kg m}^{-2} \text{ yr}^{-1} \ \& \ \text{SAR} = 3.5 \pm 0.2 \text{ mm yr}^{-1}$$

AM8: A depth of 15 ± 1 cm or 6.1 ± 0.5 g cm⁻¹ (2022-1963) corresponds to 59 ± 3 years.

MAR = 1.1 ± 0.1 kg m⁻² yr⁻¹ & SAR = 2.6 ± 0.2 mm yr⁻¹

NK7: A depth of 25 ± 1 cm or 14.53 ± 0.55 g cm⁻¹ (2021-1960) corresponds to 61 ± 5 years.

MAR = 2.4 ± 0.2 kg m⁻² yr⁻¹ & SAR = 4.1 ± 0.4 mm yr⁻¹

NK9: A depth of 29 ± 1 cm, 19.14 ± 0.85 g cm⁻¹ (2022-1961) corresponds to 61 ± 3 years.

MAR = 3.1 ± 0.2 kg m⁻² yr⁻¹ & SAR = 4.8 ± 0.3 mm yr⁻¹

An overview in table format is:

Previous values				Updated values (in line 369)			
Station	MAR (kg m ⁻² yr ⁻¹)	SAR (mm yr ⁻¹)	OCBR (g m ⁻² yr ⁻¹)	Station	MAR (kg m ⁻² yr ⁻¹)	SAR (mm yr ⁻¹)	OCBR (g m ⁻² yr ⁻¹)
GF13	14.1 ± 3.5	15.0 ± 3.7	27.5 ± 8.3	NK13	14.1 ± 3.5	15.0 ± 3.7	27.5 ± 8.3
GF12	5.9 ± 1.0	7.1 ± 1.2	9.6 ± 1.7	NK12	5.9 ± 1.0	7.1 ± 1.2	9.6 ± 1.7
GF10	7.0 ± 0.1	8.3 ± 1.1	29.4 ± 4.0	NK10	7.0 ± 0.1	8.3 ± 1.1	29.4 ± 4.0
GF9	3.4 ± 0.1	5.1 ± 1.4	19.1 ± 5.2	NK9	3.1 ± 0.2	4.8 ± 0.3	17.5 ± 0.6
GF7	2.6 ± 0.1	3.5 ± 1.3	6.5 ± 2.7	NK7	2.4 ± 0.2	4.1 ± 0.4	5.9 ± 0.8
GF6	1.8 ± 0.1	1.9 ± 0.8	1.5 ± 0.6	AM10	4.0 ± 2.8	5.2 ± 2.0	9.9 ± 5.0
AM10	4.0 ± 2.8	5.2 ± 2.0	13.1 ± 5.0	AM8	1.1 ± 0.1	2.6 ± 0.2	17.7 ± 0.3
AM8	1.1 ± 0.0	2.4 ± 0.0	17.2 ± 0.3	AM5	1.0 ± 0.1	3.5 ± 0.2	21.0 ± 1.1
AM5	1.1 ± 0.0	2.9 ± 0.3	23.9 ± 2.3				

(2) The above outcome also addresses your following concern: **“Moreover, in Table 2, AM8 and AM5 have uncertainties of 0.0.”**

As a result, average OCBR for Nuup Kangerlua and Ameralik are:

	Recalculated OCBR	Previous OCBR
Nuup Kangerlua	18.0 ± 1.6 g m ⁻² yr ⁻¹	14.1 ± 1.6 g m ⁻² yr ⁻¹
Ameralik	16.2 ± 1.7 g m ⁻² yr ⁻¹	16.5 ± 1.7 g m ⁻² yr ⁻¹

Please note that the higher value obtained for Nuup Kangerlua is mainly due to, as discussed above, the exclusion of the low MAR of station NK6.

References are:

Barsanti, M., Garcia-Tenorio, R., Schirone, A., Rozmaric, M., Ruiz-Fernández, A. C., Sanchez-Cabeza, J. A., and Osvath, I.: Challenges and limitations of the ²¹⁰Pb sediment dating method: Results from an IAEA modelling interlaboratory comparison exercise, *Quaternary Geochronology*, 59, 101093, <https://doi.org/10.1016/j.quageo.2020.101093>, 2020.

Pelikan, C., Jaussi, M., Wasmund, K., Seidenkrantz, M., Pearce, C., Kuzyk, Z. Z. A., Herbold, C. W., Røy, H., Kjeldsen, K. U., and Loy, A.: Glacial runoff promotes deep burial of sulfur cycling-associated microorganisms in marine sediments, *Frontiers in Microbiology*, 10, 2558, <https://doi.org/10.3389/fmicb.2019.02558>, 2019.

Smith J (2001) Why should we believe ^{210}Pb sediment geochronologies? *J Environ Radioact* 55: 121–123

(3) “Log transformed $^{210}\text{Pb}_{\text{ex}}$ activities were plotted against the cumulative dry mass depth (g cm^{-2}) of the sediment per station.” It would be good to show these plots.

The following figures were added to the appendix to provide more clarity on the methodology:

Line 660:

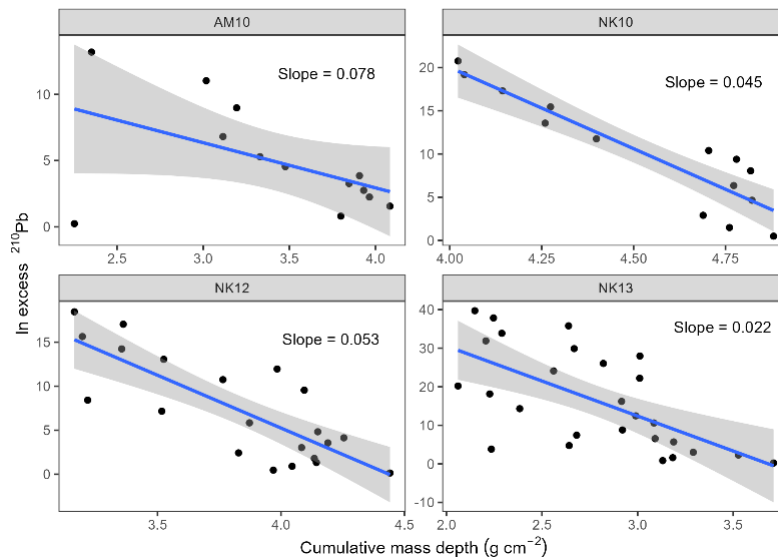


Figure A2. The natural logarithm of the activity of $^{210}\text{Pb}_{\text{ex}}$ is plotted against the cumulative mass depth with the linear blue line representing CF:CS fitting for stations AM10, NK10, 12 and 13.

Line 665:

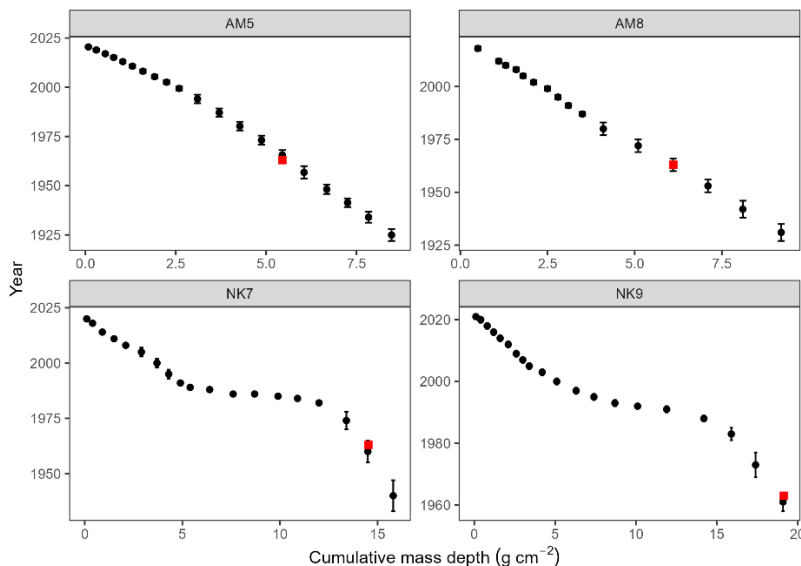


Figure A3. Age–depth models for sediment cores from stations AM5, AM8, NK7, and NK9, constructed using the Constant Rate of Supply (CRS) model based on $^{210}\text{Pb}_{\text{ex}}$ activity. Black circles represent modeled sediment ages plotted against cumulative mass depth (g cm^{-2}), with error bars showing $\pm 1\sigma$ uncertainties. Red squares indicate the depth of the ^{137}Cs activity peak (1963), used as an independent chronological marker for model validation.

(4) Also, why was the CRS model applied to some of the cores? For consistency (and if only an average sedimentation rate is required), for all cores the CF:CS model should be used.

In a very dynamic environment such as fjords with mass discharge from glaciers, we suppose that the CRS method offers a higher chance to describe the sedimentation processes. This model gave good geochronology in the cores shown in figure A3, where every ^{210}Pb age is confirmed by ^{137}Cs measurements: the average sedimentation rate calculations in AM5, AM8, NK7 and NK9 are the most robust estimates, as an additional independent tracer (^{137}Cs) could be used.

Vice versa, the absence of a clear ^{137}Cs peak in the other stations (NK10, 12, 13 and AM10) did not allow to confirm the CRS dating and, since we needed an estimate of sedimentation rate, we applied the CF:CS model. It would be indeed better to emphasize that MAR and SAR values of stations NK10, NK12, NK13 and AM10 based on CF:CS dating are estimates that should be verified in future research. Therefore, we adapted the “2.4.1 Organic carbon burial rate” section in the Materials and Methods section:

Line 261: “Log-transformed $^{210}\text{Pb}_{\text{ex}}$ activities were plotted against cumulative dry mass depth (g cm^{-2}) for each station. Sedimentation rates at stations AM5, AM8, NK7, and NK9 were determined using the constant rate of supply (CRS) model (Appleby, 2001), as a distinct increase in ^{137}Cs was detected at these sites (Fig. A1), supporting the CRS-based chronology. The observed increase in ^{137}Cs activity is attributed to global fallout from atmospheric nuclear weapons testing, which peaked in 1963. In contrast, the CF:CS (constant flux:constant sedimentation) model (Sanchez-Cabeza and Ruiz-Fernández, 2012) was applied to stations NK10, NK12, NK13, and AM10, where the $^{210}\text{Pb}_{\text{ex}}$ profiles exhibited approximately exponential trends but lacked a clearly defined ^{137}Cs peak. For these stations, log-transformed $^{210}\text{Pb}_{\text{ex}}$ activities were plotted against cumulative dry mass depth (g cm^{-2}) for each station. As a result, the sedimentation rate estimates for these stations should be treated with caution and verified in future studies. Mass accumulation rates (MAR, $\text{kg m}^{-2} \text{yr}^{-1}$) were derived from the slope of the linear regression (for CF:CS) or from the CRS model output. Bulk sediment accumulation rates (SAR, mm yr^{-1}) were calculated by

dividing MAR by the average bulk density at each station. Organic carbon burial rates (OCBRs) were then calculated by multiplying MAR by the TOC content at the 9 – 10 cm sediment layer.”

(5) Furthermore, how was the lack of bioturbation determined? From the Cs profiles in Fig. A1, it does look as if mixing may have affected at least some of the cores.

We stated “No bioturbated or mixed upper layer was observed in the profiles.” This indeed required a more elaborated explanation and was changed to (lines 281-288): “We did not apply corrections for bioturbation or mixing processes, as the $^{210}\text{Pb}_{\text{ex}}$ profiles do not show evidence of such activity in the upper sediment layers. However, these processes cannot be conclusively ruled out, particularly since some of the ^{137}Cs profiles feature broad activity peaks. Nonetheless, the ^{210}Pb -derived chronology appears to be supported by the ^{137}Cs profiles in AM5, AM8, NK7 and NK9 (Smith, 2001; Barsanti et al., 2020). The broad ^{137}Cs curves or inflections, marking sustained elevation in ^{137}Cs activity after an initial increase followed by a gradual decrease over time, are therefore more likely explained by continued exposure of settling particles to residual ^{137}Cs in the overlying water after 1963. As a result, younger sediment layers also contain measurable amounts of ^{137}Cs , smearing the signal across multiple horizons. This phenomenon has been observed in other marine settings (Tamburrino et al. 2019) and even in lake sediments (Drexler et al., 2018).

Following references were added to the reference list:

Barsanti, M., Garcia-Tenorio, R., Schirone, A., Rozmaric, M., Ruiz-Fernández, A. C., Sanchez-Cabeza, J. A., and Osvath, I.: Challenges and limitations of the ^{210}Pb sediment dating method: Results from an IAEA modelling interlaboratory comparison exercise, *Quaternary Geochronology*, 59, 101093, <https://doi.org/10.1016/j.quageo.2020.101093>, 2020.

Drexler, J. Z., Fuller, C. C., and Archfield, S.: The approaching obsolescence of ^{137}Cs dating of wetland soils in North America, *Quaternary Science Reviews*, 199, 83–96, <https://doi.org/10.1016/j.quascirev.2018.08.028>, 2018.

Smith, J. N.: Why should we believe ^{210}Pb sediment geochronologies?, *Journal of Environmental Radioactivity*, 55, 121–123, [https://doi.org/10.1016/S0265-931X\(01\)00110-2](https://doi.org/10.1016/S0265-931X(01)00110-2), 2001.

Tamburrino, S., Passaro, S., Barsanti, M., Schirone, A., Delbono, I., Conte, F., Delfanti, R., Bonsignore, M., Del Core, M., Gherardi, S., en Sprovieri, M.: Pathways of inorganic and organic contaminants from land to deep sea: The case study of the Gulf of Cagliari (W Tyrrhenian Sea), *The Science Of The Total Environment*, 647, 334–341, <https://doi.org/10.1016/j.scitotenv.2018.07.467>, 2019.

(6) Another, smaller point: the authors state that their findings regarding higher OC content in the LTG fjord came as a surprise – yet comparisons with literature data (Figure 5) reveal that this is not so different from earlier studies in other regions.

Taking into account your remark, we rephrased (lines 391-398) within the discussion: “So far, studies comparing MTG and LTG fjord systems are limited (Koziorowska et al., 2015; Laufer-Meiser et al., 2021). These studies suggest that MTG fjords tend to exhibit higher OC accumulation, as indicated by elevated OC content in surface sediments. However, when comparing the LTG system Ameralik and the MTG system Nuup Kangerlua with datasets from other fjords (Smith et al., 2002; Thamdrup et al., 2007; Koziorowska et al., 2015; Cui et al., 2016; Faust and Knies, 2019; Włodarska-Kowalczyk et al., 2019; Laufer-Meiser et al., 2021), we observed that surface sediment OC content in LTG and even non-glaciated fjords can be comparable to that of MTG systems across the (sub-)Arctic region (Fig. 5A).

Nevertheless, it is important to note that LTG fjords are underrepresented in current datasets, and low-glacial-activity MTG systems may bias comparative interpretations.”

(7) Abstract: The last two sentences could be combined as they are a bit redundant at the moment. The available space could then be allocated to mention e.g. results for OC composition or provide more detail (orders of magnitude) for sedimentation rates and/or OCBR, or some info on which parameters were measured for this study.

Good point. We applied your comment in:

Line 17: This study compares sediment TOC, TN, and Chl-a content as well as $\delta^{13}\text{C}$, $\delta^{15}\text{N}$ and organic carbon burial rates (OCBRs) in two neighbouring Greenland fjords, Nuup Kangerlua, influenced by marine-terminating glaciers (MTGs), and Ameralik, dominated by land-terminating glaciers (LTGs), to explore the effects of both types of glaciers on sediment carbon dynamics.

Line 24: Despite different glacial regimes, the two investigated fjord systems showed similar traits with OC predominantly of marine origin and similar OCBRs of 18.0 ± 1.6 and $16.2 \pm 1.7 \text{ g m}^{-2} \text{ yr}^{-1}$ in Nuup Kangerlua and Ameralik, respectively. Higher Chl-a and OC contents were recorded in the sediments of outer and mid Ameralik compared to those in Nuup Kangerlua. The results underscore that benthic – pelagic coupling in glacial fjords is complex, emphasizing the need for further research to disentangle the interactions driving primary production, lateral and vertical OC transport, as well as OC degradation and preservation in fjord sediments.

(8) Figure 1: Sample IDs could be shown on the map.

We improved Figure 1 (**line 122**) based on your comment and the other two reviewers by:

- Adding a legend, depicting stations sampled in Nuup Kangerlua and stations in Ameralik in a different color.
- Adding station labels and adjusting the symbol of Nuuk to differentiate it from the station symbols.
- Situating the outer, mid and inner zone in the (b) panel.
- Enlarging (a) and (b) panel.

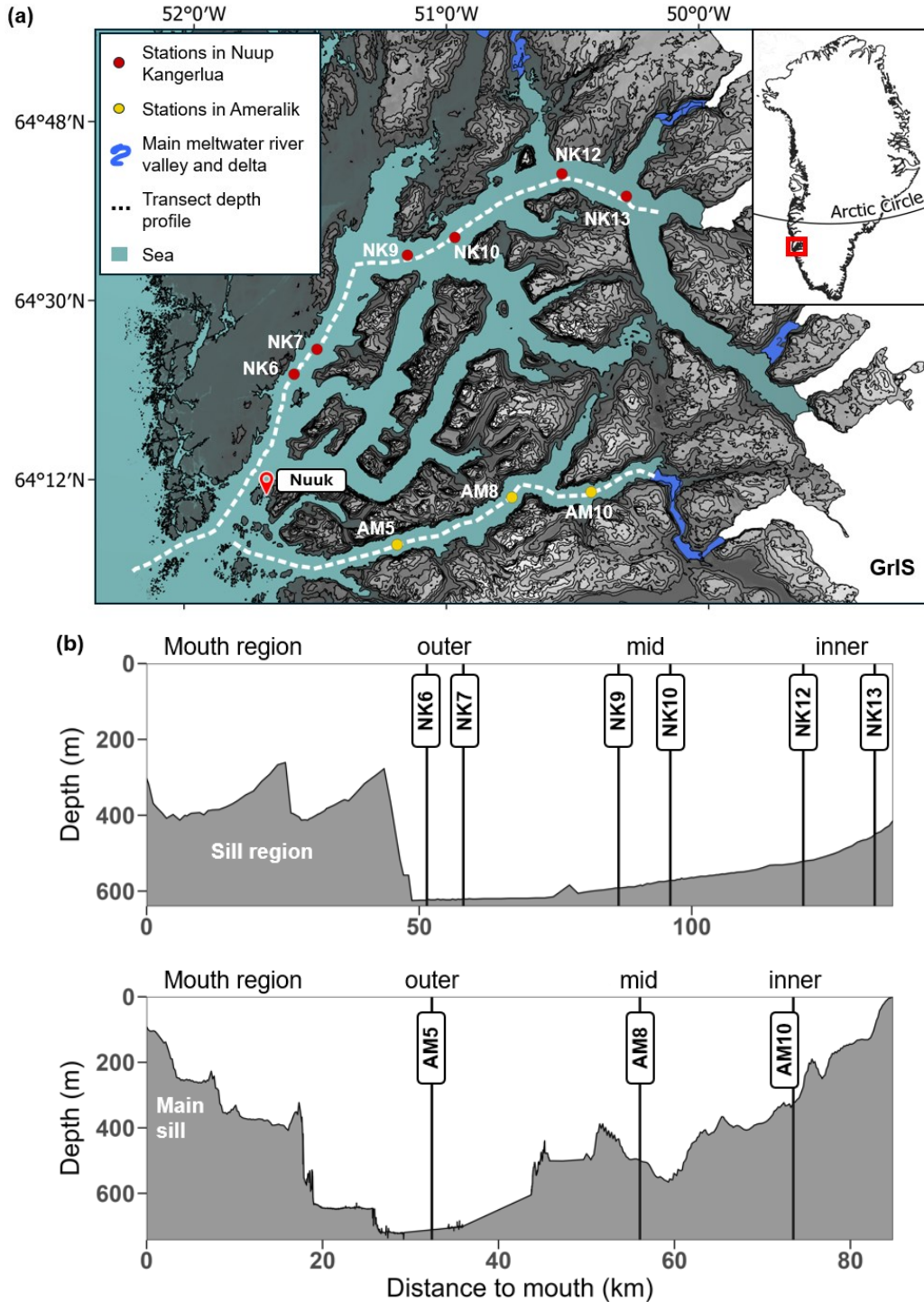


Figure 1. (a) Map showing sampling locations in Nuup Kangerlua (fed by three marine-terminating glaciers and three land-terminating glaciers) and Ameralik (receiving meltwater from a land-terminating glacier). Greenland Ice Sheet (GrIS) is depicted in white. (b) Water depth profiles along-axis (white dashed lines) Nuup Kangerlua (top) and Ameralik (bottom). Both fjord basins are divided in an outer, mid and inner section behind the entrance sill(s).

(9) Figure 4: A second panel with C:N vs $\delta^{13}\text{C}$ could be added, as C:N ratios have also been commonly employed to distinguish terrestrial from marine OC.

Thank you for this insightful suggestion. We agree that plotting $\delta^{13}\text{C}$ against C:N ratios adds value, as both are commonly used to distinguish between terrestrial and marine organic carbon sources. We have therefore revised Figure 4 (line 358) including other remarks of other reviewers. We improved this figure by:

- Enlarging all elements of the figure.
- Adding a second panel, displaying $\delta^{13}\text{C}$ against C:N ratio. We indicated the marine and terrestrial end-member $\delta^{13}\text{C}$ values used in this study to determine the proportion of marine and terrestrial OC.
- Colors referring to Nuup Kangerlua and Ameralik were adapted to follow the color code of the map (Figure 1; line 122).
- In panel (a), we extended the marine and terrestrial ranges from $\delta^{13}\text{C}$ -23 ‰ to $\delta^{13}\text{C}$ -24‰ and from $\delta^{15}\text{N}$ -25 ‰ to $\delta^{15}\text{N}$ -21‰ (following Lamb et al., 2006), respectively.

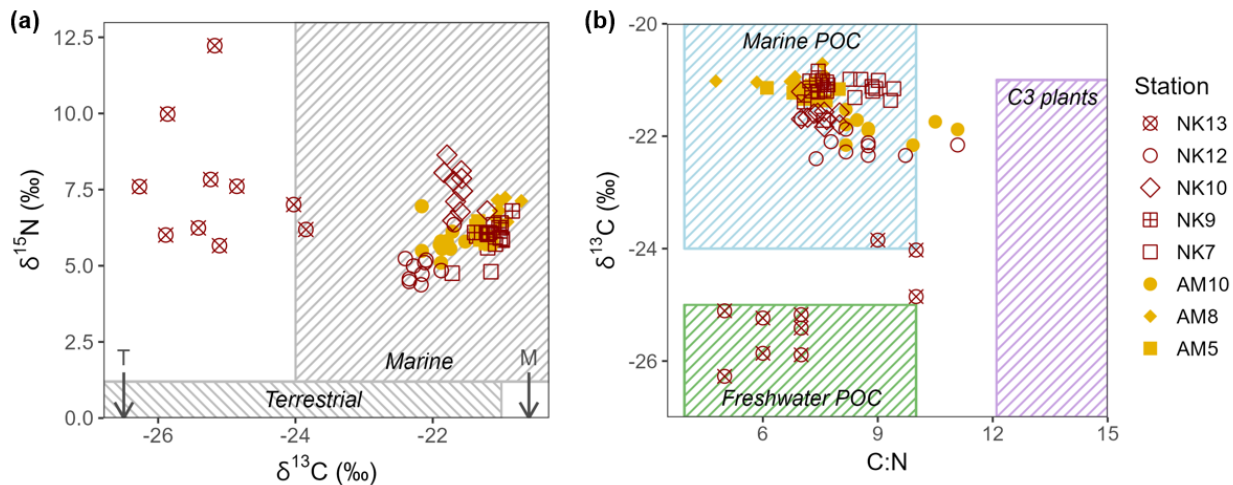


Figure 4. (a) $\delta^{13}\text{C}$ (‰ deviations from V-PDB) values plotted against $\delta^{15}\text{N}$ (‰ deviations from air) values of the POM present in the sediment for the different station of Ameralik (filled symbols) and Nuup Kangerlua (open symbols). Typical marine and terrestrial ranges of $\delta^{13}\text{C}$ (Lamb et al., 2006) and $\delta^{15}\text{N}$ (Zaborska et al., 2018) are indicated with rectangles. (b) $\delta^{13}\text{C}$ plotted against C:N ratios. Ranges of marine and freshwater POC, and C3 terrestrial plants are displayed as rectangles for reference (values taken from Lamb et al., 2006). Marine (M) and terrestrial (T) $\delta^{13}\text{C}$ end-members used in this study are indicated with arrows.

In addition we added to the text, section “2.3.1 Calculation of marine organic carbon fraction”: lines 212 – 219: Stable isotope composition in addition to C:N ratios of settled organic matter in fjord sediments has been used in multiple studies to estimate the proportion of marine versus terrestrially derived organic matter (St-Onge and Hillaire-Marcel, 2001; Koziarowska et al., 2015; Smeaton & Austin, 2017; Zaborska et al., 2018; Faust and Knies, 2019; Limoges et al., 2020; Placitu et al., 2024). Terrestrial organic matter, primarily derived from vascular plants, tends to have higher C:N ratios (> 12) and more depleted $\delta^{13}\text{C}$ values (-25 to -30 ‰ $\delta^{13}\text{C}$) due to the dominance of lignin-rich, cellulose-based material and the use of C3 photosynthesis pathways (Lamb et al., 2006). In contrast, marine organic matter, originating from phytoplankton and other aquatic organisms, typically shows lower C:N ratios and less negative $\delta^{13}\text{C}$ values (-18 to -24 ‰ $\delta^{13}\text{C}$), reflecting a protein-rich composition and different carbon fixation mechanisms (Lamb et al., 2006).

- (10) **L161-170: For the proportions of terrestrial vs marine OC, the selection of endmember values need more explanation: “These end-members were derived from Northern and Mid-Norway fjord sediments” – how? Also, those values should have some uncertainties, which would then propagate to the fraction estimates. In Figure 4, the endmembers appear to have uncertainties.**

We added the following to the “2.3.1 Calculation of marine organic carbon fraction section”: **Lines 227-234**: The catchments of both fjords consist of tundra shrub vegetation, which are typically C₃ plants. Published $\delta^{13}\text{C}$ values for terrestrial plant material in Greenland remain limited, but available data indicate a range of -33.9‰ to -26.9‰ (Thompson et al., 2018). However, due to the scarcity of $\delta^{13}\text{C}$ records specific to Greenland’s marine organic matter, terrestrial vegetation and soil, we adopted end-member values from nearby Arctic and sub-Arctic systems. For the marine end-member, we used a $\delta^{13}\text{C}$ value of -20.6‰, consistent with those reported in Svalbard studies by Winkelman and Knies, and Koziorowska et al. (2015). We used the marine end-member value from Faust and Knies (2019), originally applied in sub-Arctic Norwegian fjords, as it falls within the broader $\delta^{13}\text{C}$ range of Arctic terrestrial organic matter (-35‰ to -25‰) reported by Kuliński et al. (2014).

The data derived from these publications did not contain uncertainty estimates, but we used the reported values to indicate the range of end-member values (dashed zones in figure 4).

We added following references:

Limoges, A., Weckström, K., Ribeiro, S., Georgiadis, E., Hansen, K. E., Martinez, P., Seidenkrantz, M., Giraudeau, J., Crosta, X., en Massé, G.: Learning from the past: Impact of the Arctic Oscillation on sea ice and marine productivity off northwest Greenland over the last 9,000 years, *Global Change Biology*, 26, 6767–6786, <https://doi.org/10.1111/gcb.15334>, 2020.

Thompson, H. A., White, J. R., and Pratt, L. M.: Spatial variation in stable isotopic composition of organic matter of macrophytes and sediments from a small Arctic lake in west Greenland, *Arctic Antarctic And Alpine Research*, 50, <https://doi.org/10.1080/15230430.2017.1420282>, 2018.

St-Onge, G. and Hillaire-Marcel, C.: Isotopic constraints of sedimentary inputs and organic carbon burial rates in the Saguenay Fjord, Quebec, *Marine Geology*, 176, 1–22, [https://doi.org/10.1016/s0025-3227\(01\)00150-5](https://doi.org/10.1016/s0025-3227(01)00150-5), 2001.

Technical corrections:

- (11) **Short summary: “necessarily” instead of “necessary”**

Adjusted in the text.

- (12) **Abstract: L21, 23 & 25 “organic carbon” should be “OC”**

Adjusted in the text.

- (13) **Figure A2: In the caption, it reads “Orange and black colors represent end of summer 2021 and spring 2022”, yet there is no orange in the figure.**

Figure caption changed to: “... Grey and black colors represent end of summer 2021 and spring 2022, respectively. Data from the two seasons is available for stations NK12, NK7, AM10 and AM5.” (**Line 665**).

Based on comments of other two reviewers, we reformulated large parts of the discussion and we reorganized it according to the following structure:

- **4.1 Surface sediment OC content** with a sub-section on **OC origin** (4.2.1), putting more emphasis on what can be derived from our data.
- **4.2 Organic carbon burial rates**, which was set as the 2nd sub section instead of the last paragraph. We also included primary production values from literature.
- We assembled our 3 main hypotheses in sub-sections within **4.3 Pelagic and geomorphological influence on OC burial**:
 - o **4.3.1 OC preservation conditions**, which was condensed and more focused on the bottom water temperature differences we measured between the fjords. We removed the hypothesis regarding a difference in OC preservation related to Fe and Mn in both fjords from the discussion due to limited data to support this hypothesis.
 - o We condensed section **4.3.2 Transport dynamics**. This section was included to provide a more nuanced view of MTG-induced upwelling, acknowledging that nutrient enrichment may also originate from upwelling at the fjord mouth, potentially influencing the patterns observed in our study
 - o We condensed the **4.3.3 Food web OC uptake** section.
- We incorporated the suggestion of Anonymous Referee #1 to add a section on Recommendations for future research.

To avoid an overly long rebuttal letter, we refer the reviewer to our rewritten discussion in the manuscript. (From line **371** onwards).